Laboratory Astrophysics: Measurements of $n=n'$ to $n=2$ Line Emission in Fe^{16+} to Fe^{23+}

D. W. Savin*, P. Beiersdorfer[†], G. V. Brown[‡], J. Crespo López-Urrutia[†], V. Decaux[†], S. M. Kahn[§], D. A. Liedahl[†], K. J. Reed[†], and K. Widmann[†]

*Space Sciences Laboratory, 366 LeConte, University of California, Berkeley, CA 94720
[†]Department of Physics and Space Technology, Lawrence Livermore National Laboratory, University of California, Livermore, CA 94550
[‡]Department of Physics, Auburn University, Auburn, AL 36849
[§]Department of Physics, Columbia University, New York, NY 10027

Abstract. One of the dominant forms of astronomical line emission in the 6 Å to 18 Å spectral region is line emission produced by $n=n'$ to $n=2$ transitions in Fe^{16+} to Fe^{23+} (*i.e.*, Fe *L*-shell n-2 line emission). Using the Lawrence Livermore National Laboratory electron beam ion trap (EBIT) facility, we have carried out a number of measurements designed to address astrophysical issues concerning Fe *L*-shell line emission. Desired ions are produced and trapped using the nearly monoenergetic electron beam of EBIT. Trapped ions are collisionally excited and the resulting X-ray line emission detected using Bragg crystal spectrometers. We have recently completed a line survey of Fe *L*-shell 3-2 line emission. The line survey will allow a more reliable accounting of line blending in astronomical spectra. We have now begun a series of broadband, high resolution line ratio measurements. These measurements are designed to benchmark atomic calculations used in astronomical plasma emission codes and also for comparison with X-ray spectral observations of astronomical objects. Initial measurements have been carried out in Fe^{23+}. Preliminary results agree with distorted wave calculations to within 20 percent and better.

INTRODUCTION

In astronomical plasmas, transitions in the iron *L*-shell ions (Fe^{16+} to Fe^{23+}) of the type $n=n'$ to $n=2$ (hereafter, n'-2) are one of the dominant forms of line emission in the 6 Å to 18 Å spectral region. Iron L-shell line emission (*i.e.*, *n*-2) is seen in spectra from the sun (1,2), other stars (3,4), supernova remnants (5), cataclysmic variables (6), X-ray binaries (7), active galactic nuclei (8), and clusters of galaxies (9). Astrophysical interpretation of these spectra, however, are compromised by fundamental uncertainties that still remain in our understanding of the basic atomic physics processes that generate the observed X-ray spectra. Two examples serve to demonstrate this point.

The first example involves a long standing problem in solar observations. *L*-shell lines from neonlike Fe^{16+} are among the most intense X-ray lines emitted from the solar corona. These line are observed both in the presence and in the absence of flares (2). The observed Fe^{16+} line ratios, however, do not agree with theoretical predictions for inferred coronal temperatures. A number of different solar physics and atomic physics explanations have been put forward in an attempt to explain the apparent discrepancies. Possible solar physics explanations include resonant scattering of the strongest Fe^{16+} lines (2) or explosive events in the corona producing ionizing plasmas (10). Possible atomic physics explanations have been addressed by carrying out new, more detailed atomic calculations (11-13). The resolution of these discrepancies may have major implications for solar physics. If the explanation is resonant scattering, then that may offer the possibility of a new density diagnostic (14,15). And if explosive events are the explanation, then that would have implications for the heating of the solar corona (10). Laboratory benchmark measurements can aid greatly in resolving the apparent Fe^{16+} line ratio discrepancies and addressing the associated solar physics issues.

The second example involves a recent observation by the *Advanced Satellite for Cosmology and Astrophysics* (*ASCA*) of cooling flows in the Centaurus cluster of galaxies (9). The launching of *ASCA* in 1993 of the has opened a new era in high energy astrophysics. The large collecting area and moderate spectral resolving power of the spectrometers on *ASCA* are yielding high signal-to-noise X-ray spectra of many extrasolar astronomical objects (16). These spectra challenge the quality of the atomic data used in existing standard plasma emission codes. For example, in the 8 Å to 18 Å spectral band, significant discrepancies exist between *ASCA* observations of cooling flows in the Centaurus cluster of galaxies and model spectra from plasma emission codes (9). These discrepancies cannot be eliminated by invoking multi-temperature, multi-density distributions, nor by varying relative elemental abundances. Because cooling flows are believed to be optically thin, quasi-static plasmas (17), other astrophysical effects are expected to be insignificant. Hence, the discrepancies indicate the existence of errors in the atomic data used in the plasma codes, and have been attributed to errors in the electron impact excitation (EIE) rate coefficients for producing *n*-2 line emission in Fe^{22+} and Fe^{23+} (18).

The importance of accurate atomic data for *n*-2 transitions in iron *L*-shell ions is not limited just to *ASCA* or solar spectra. The planned launches later this decade of the *Advanced X-Ray Astrophysics Facility* (*AXAF*, 19), the *X-Ray Multimirror Mission* (*XMM*, 21) and *ASTRO-E* (22) will put in orbit spectrometers which will collect extrasolar spectra in the 6 Å to 18 Å spectral band with resolving powers, $\lambda/\Delta\lambda$, over an order of magnitude greater than those of *ASCA* spectrometers. Interpreting *AXAF*, *XMM*, and *ASTRO-E* spectra will, therefore, require atomic data with an accuracy and completeness significantly greater than exists at the present time.

For several years, we have been carrying out experimental measurements of *n*-2 line emission from the iron *L*-shell ions in order to address these present and future needs of high energy astrophysics. Measurements are carried out using the Lawrence Livermore National Laboratory electron beam ion trap (EBIT) facility (22,23). Iron ions of interest are produced, trapped, and excited by collisions with the nearly monoenergetic electron beam in EBIT. The emitted *L*-shell X-ray lines are recorded and analyzed with high resolution Bragg crystal spectrometers (24).

ELECTRON BEAM ION TRAP MEASUREMENTS

Line Surveys

Iron *L*-shell line emission is comprised of numerous strong transitions which, depending on the temperature of the emitting source, result typically from transitions in Fe^{14+} to Fe^{23+}. The analysis of iron *L*-shell spectra thus requires consideration of a large number of ionization stages and a large number of possible transitions. A reliable analysis of astronomical spectra must account for all lines and needs to employ accurate line position information to properly model line blending. To address these issues, we have made a survey of the iron *L*-shell 3-2 transitions in the 10 Å to 17.5 Å spectral range. A representative Fe^{16+} *L*-shell spectrum is shown in Fig. 1 (24). Spectra were collected from Fe^{16+} through to Fe^{23+} (25). Charge balances consisting primarily of a single ionization stage of iron were produced in EBIT by setting the electron beam energy to just below the ionization threshold for the charge state of interest. This allowed observed spectral lines to be unambiguously assigned to a given ionization stage of iron. The wavelength scale was determined by observing *K*-shell (*i.e.*, *n*-1) transitions in hydrogenlike and heliumlike oxygen, fluorine, neon, and magnesium. An accuracy of about 0.1-0.3 eV was achieved in the determination of the transition energies. For example, the measured wavelength of 3E, the weakest Fe^{16+} line in Fig. 1, was 15.456±0.004 Å while that of 3C, the strongest line, was 15.009±0.001 Å (24). Identifications of lines in the higher charge states of iron that have not been identified in earlier measurements were made by comparing observed intensities and measured wavelength with calculations from a collisional-radiative model which uses the Hebrew University-Lawrence Livermore set of atomic codes (HULLAC, 26,27).

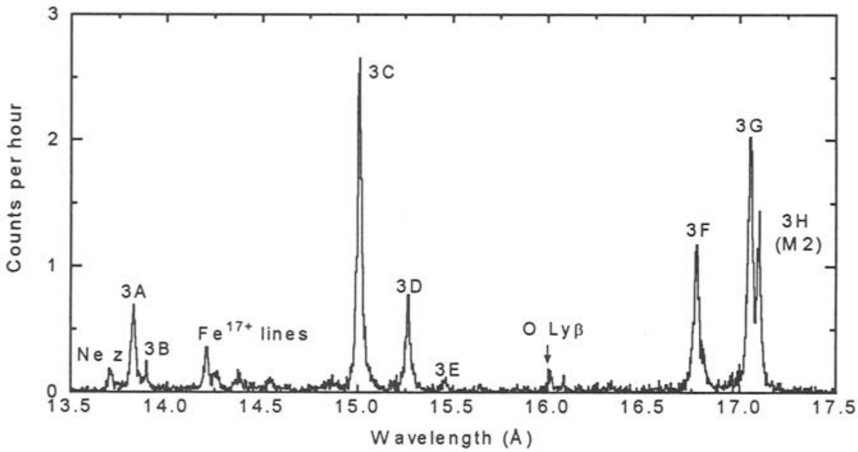

Figure 1. Fe^{16+} *L*-shell spectrum recorded using a thallium hydrogen phthalate crystal in first order. The electron beam energy was 1300 eV. The spectrum is a composite of data from three different crystal settings. Fe^{16+} lines are labeled using the notation of Ref. 1.

Line Ratio Measurements

X-ray spectral observations of astronomical objects are typically broadband. To be useful, laboratory measurements must, accordingly, be broadband. And for comparison with atomic calculations it is necessary to collect spectra at a resolving power high enough that individual observed spectral lines are fully resolved. These two requirements, broadband spectra with high resolving power, have been met by using two crystal spectrometers to observe simultaneously line emission from EBIT. Crystal spectrometers, however, are inherently narrowband devices with X-ray detection efficiencies which over a broad band may change dramatically. Broadband line ratio measurements are carried out by using the two spectrometers to observe simultaneously different narrowband regions (each containing lines of interest).

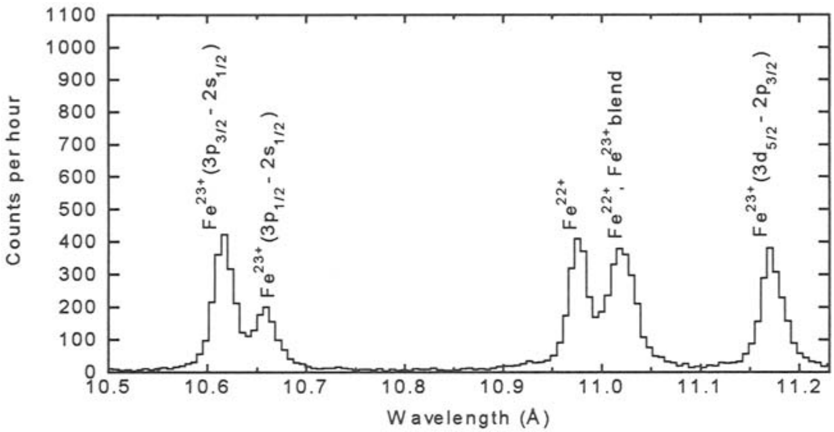

Figure 2. Iron *L*-shell 3-2 spectrum recorded using a thallium hydrogen phthalate crystal in first order. The electron beam energy was 4500 eV.

The ion selected for our initial broadband line ratio measurements was Fe^{23+} This ion was chosen for a number of reasons. Fe^{23+} is lithiumlike which makes it a relatively simple ion to work with both experimentally and theoretically. This makes Fe^{23+} a good initial test-case for carrying out quantifiable, broadband line ratio measurements. And astrophysically, Fe^{23+} was chosen to provide benchmark measurements for the HULLAC calculations (18) which appear largely to remove the reported (8) discrepancies between *ASCA* observations of the Centaurus cluster of galaxies and predictions from plasma emission codes.

For our initial experiments we have measured the EIE-generated Fe^{23+} $(3p_{3/2}$-$2s_{1/2})/(3p_{1/2}$-$2s_{1/2})$, $(3d_{5/2}$-$2p_{3/2})/(3p_{1/2}$-$2s_{1/2})$, and $(4p_{3/2,1/2}$-$2s_{1/2})/(3p_{1/2}$-$2s_{1/2})$ line ratios (28). Representative Fe^{23+} spectra are shown in Figs. 2 and 3. Measurements have been carried out at electron beam energies of 2.5 and 4.5 keV. These energies are above the ionization potential for Fe^{23+}, which ensures that the measured line ratios are due solely to EIE and are free of any contributions from dielectronic recombination. At these beam energies, significant amounts of Fe^{24+} exist in EBIT. Recombination-cascade contributions due to radiative recombination of Fe^{24+} with beam electrons and from charge transfer of Fe^{24+} with background gas in EBIT were determined to have an insignificant effect on the measured line intensities. EBIT uses a directed beam of electrons which can produce anisotropically emitted, linear polarized radiation (29). These effects on the measured line intensities were accounted for using the formalism of Ref. (30) combined with distorted wave calculations using the code of Ref. (31).

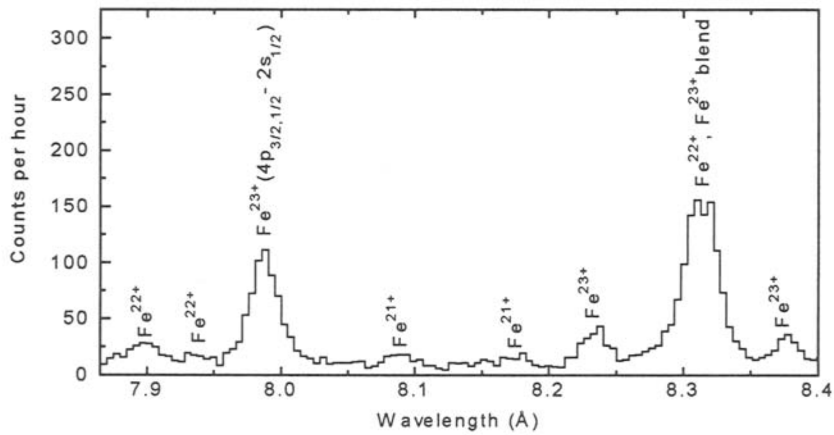

Figure 3. Iron *L*-shell 4-2 spectrum recorded using a thallium hydrogen phthalate crystal in first order. The electron beam energy was 4500 eV.

The X-ray detection efficiency for one of the crystal spectrometers was established by calibrating the thin foil windows and thallium acid phthalate crystal used for the present measurements. X-rays were detected in the spectrometer using a flowing gas proportional counter (FGPC) with an absorbing gas of 90% Ar and 10% CH_4 (24). X-ray detection efficiencies were calculated from the measured depth of the FGPC gas volume and using photoabsorption cross sections which are well known experimentally and theoretically (32). The narrow band

$(3p_{3/2}\text{-}2s_{1/2})/(3p_{1/2}\text{-}2s_{1/2})$ and $(3d_{5/2}\text{-}2p_{3/2})/(3p_{1/2}\text{-}2s_{1/2})$ line ratios were measured using the calibrated spectrometer. The broad band $(4p_{3/2,1/2}\text{-}2s_{1/2})/(3p_{1/2}\text{-}2s_{1/2})$ line ratio was measured using both spectrometers. The uncalibrated spectrometer was cross-calibrated with the calibrated spectrometer for detection of the $3p_{1/2}\text{-}2s_{1/2}$ line by simultaneously observing this line with both spectrometers. The $(4p_{3/2,1/2}\text{-}2s_{1/2})/(3p_{1/2}\text{-}2s_{1/2})$ line ratio was measured using the calibrated spectrometer to observe the $4p_{3/2,1/2}\text{-}2s_{1/2}$ line and the cross-calibrated spectrometer to observe the $3p_{1/2}\text{-}2s_{1/2}$ line.

A preliminary data analysis indicates that the measured line ratios and predictions by HULLAC and by the distorted wave code of Ref. (31) all agree to within 20 percent and better. For example, the measured $(4p_{3/2,1/2}\text{-}2s_{1/2})/(3p_{1/2}\text{-}2s_{1/2})$ line ratio at 4.5 keV is $0.492\pm0.074(1\sigma)$ while the ratio predicted by HULLAC is 0.409 and by the code of Ref (31) is 0.386. The uncertainty quoted here represents the total experimental uncertainty in the measured line ratio. The accuracies of the present line ratio measurements are limited by the resolving powers of the crystal spectrometers and the resulting uncertainty in determining the background level in collected spectra. The spectra shown in Figs. 2 and 3 were collected at a resolving power of 500. Future measurements will be carried out using spectrometers with resolving powers in excess of 1000.

CONCLUSIONS

Using EBIT we have carried out a number of measurements of iron *L*-shell line emission designed to address astrophysical issues. Our recently completed line survey will allow a more reliable accounting of line blending in astronomical spectra. More recently, we have demonstrated that broadband, high resolution, iron *L*-shell line ratio measurements can be carried out using EBIT. These iron *L*-shell line ratio measurements are the beginning of a series of measurements which will benchmark atomic calculations used in plasma emission codes and also be used for comparison with X-ray spectral observations of astronomical objects.

ACKNOWLEDGEMENTS

This work was performed under the auspices of the U. S. Department of Energy by the Lawrence Livermore National Laboratory under contract number

W-7405-ENG-48 and supported by NASA High Energy Astrophysics X-Ray Astronomy Research and Analysis grant NAGW-4185.

REFERENCES

1. Parkinson, J. H., *Astron. Astrophys.* **24**, 215-218 (1973).
2. Rugge, H. R. and McKenzie, D. L., *Astrophys. J.* **297**, 338-346 (1985).
3. Vedder, P. W. and Canizares, C. R., *Astrophys. J.* **270**, 666-670 (1983).
4. Agrawal, P. C. *et al.*, *Mon. Not. R. Astron. Soc.* **213**, 761-771 (1985).
5. Winkler, P. F. *et al.*, *Astrophys. J.* **246**, L27-L31 (1981).
6. Mauche, C. W. and Raymond, J. C., in *New Horizon of X-Ray Astronomy*, edited by F. Kamino and T. Ohashi, Tokyo: Univeral Academy Press, Inc., 1994, pp 399-400.
7. Kahn, S. M., Seward, F. D, and Chlebowski, T., *Astrophys. J.* **283**, 286-294 (1984).
8. Iwasawa, I. *et al.*, *Publ. Astron. Soc. Japan* **46**, L167-L171 (1994).
9. Fabian, A. C. *et al.*, *Astrophys. J.* **436**, L63-L66 (1994).
10. Feldman, U., *Comm. At. Mol. Phys.*, **31**, 11-20 (1995).
11. Raymond, J. C. and Smith, B. W., *Astrophys. J.* **306**, 762-766 (1986).
12. Chen, M. H. and Reed, K. J., *Phys. Rev. A* **40**, 2292-2300 (1989).
13. Goldstein, W. H. *et al.*, *Astrophys. J.* **344**, L37-L40 (1989).
14. Schmelz, J. T., Saba, J. L. R., and Strong, K. T., *Astrophys. J.* **398**, L115-L118 (1992).
15. Waljeski, K. *et al.*, *Astrophys. J.* **429**, 909-923 (1994).
16. Tanaka, Y. Inoue, H, and Holt, S. M., *Publ. Astron. Soc. Japan* **46**, L37-L41 (1994).
17. Fabian, A. C., *Ann. Rev. Astron. Astrophys.* **32**, 277-318 (1994).
18. Liedahl, D. A., Osterheld, A. L., and Goldstein, W. H., *Astrophys. J.* **438**, L115-L118 (1995).
19. Markert, T. H., in *UV and X-ray Spectroscopy of Laboratory and Astrophysical Plasmas*, by E. Silver and S. M. Kahn, eds., Cambridge: Cambridge University Press, 1993, pp. 459-468.
20. Brinkman, A. C., in *UV and X-ray Spectroscopy of Laboratory and Astrophysical Plasmas*, E. Silver and S. M. Kahn, eds., Cambridge: Cambridge University Press, 1993, pp. 469-482.
21. http://www.astro.isas.ac.jp/xray/mission/astroe/astroeE.html.
22. Levine, M. A. *et al.*, *Physica Scripta* **T22**, 157-163 (1988).
23. Levine, M. A. *et al.*, *Nucl. Instrum. Methods* **B43**, 431-440 (1989).
24. Beiersdorfer, P. and Wargelin, B. J., *Rev. Sci. Instrum.* **65**, 13-17 (1994).
25. Brown, G. V. *et al.* (in preparation).
26. Klapisch, M. *et al.*, *J. Opt. Soc. Am.* **67**, 148-155, (1977).
27. Bar-Shalom, A., Klapisch, M., and Oreg, J., *Phys. Rev. A* **38**, 1773-1784 (1988).
28. Savin, D. W. *et al.* (in preparation).
29. Percival, I. C. and Seaton, M. J., *Phil. Trans. Roy. Soc. London Ser. A* **251**, 113-138.
30. Steffen, R. M. and Alder, K. in *The Electromagnetic Interaction in Nuclear Spectroscopy*, edited by W. D. Hamilton, Amsterdam, North-Holland Publishing Company, 1975, ch. 12.
31. Zhang, H. L., Sampson, D. H., and Clark, R. E. H., *Phys. Rev. A* **41**, 198-206 (1990).
32. Henke, B. L. Gullikson, E. M., and Davis, J. C., *At. Data Nucl. Data Tables*, **54**, 181-342 (1993).